# Shape control with the XSC during plasma current ramp-up and ramp-down at the JET tokamak

G. De Tommasi, G. Ambrosino, M. Ariola, G. Calabrò, S. Galeani, F. Maviglia, A. Pironti,
F. G. Rimini, A. C. C. Sips, G. Varano, R. Vitelli, L. Zaccarian and JET-EFDA Contributors*

*Abstract*— The eXtreme Shape Controller (XSC) has been originally designed to control the plasma shape at JET during the flat-top phase, when the plasma current has a constant value. During the JET 2012 experimental campaigns, the XSC has been used to improve the shape control during the transient phases of plasma current ramp-up and ramp-down. In order to avoid the saturation of the actuators with these transient phases, a Current Limit Avoidance system (CLA) has been designed and implemented. This paper discusses the CLA algorithm and presents the experimental results achieved at JET during the 2012 campaigns using the XSC.

Keywords: Tokamak control; Plasma shape control; eXtreme Shape Controller; Current Limit Avoidance.

## I. INTRODUCTION

IN tokamak fusion devices the plasma shape control system plays an essential role. Indeed, an accurate plasma-boundary control is needed to obtain the vertical elongated plasmas required in the so-called advanced scenarios. Furthermore, plasma shape control is essential to optimize the coupling with the additional heating systems, to avoid plasma wall interactions, and to optimize the divertor shape for pumping.

The eXtreme Shape Controller (XSC) has been originally designed and developed at JET in 2003 to achieve a better control of the plasma shape [1]. The XSC controls the whole plasma boundary minimizing the error on more than 30 plasma shape geometrical descriptors (gaps, strike points and X-point); thus it can be used to obtain high performance plasmas. The XSC control algorithm is based on a singular

value decomposition of the plasma model at the steady state, and it enables one to minimize the control error in the least-mean-square sense for non-right invertible plants [2]. This approach has proven to be effective at JET [3] and it has been recently adopted also for plasma internal profile control in [4].

The original XSC design algorithm does not explicitly take into account the current saturation limits of the control coils. In order to overcome this limitation, the Current Limit Avoidance System (CLA) has been designed and implemented at the JET tokamak in 2011 [5], [6]. The CLA keeps the control currents within their limits without degrading the plasma shape too much, by finding an optimal trade-off between these two objectives.

Adoption of the CLA has made the plasma operations safer, and therefore the XSC has become more widely used. As an example, although the XSC is available at JET since 2003, in 2012 the pulse #83014 has been the first pulse ever to be *entirely controlled* by the XSC. Furthermore, using the CLA, it has been possible to exploit the XSC in order to control the plasma shape better during both the plasma current ramp-up and ramp-down. Indeed, during these transient phases some control currents are close to their saturation limits, hence the adoption of the CLA makes the XSC operation safer with respect to what has been done in the past.

This paper discusses on the experiments carried out at JET during the 2012 *ITER-like wall* campaigns. In particular, it focuses on the improvements in plasma shape control performance achieved by using the XSC with the CLA during both the plasma current ramp-up and ramp-down phases. The next section gives a general overview of the JET Plasma Position and Current Control System, while Section III briefly introduces both the XSC and CLA control algorithms. The experimental results achieved during the 2012 experimental campaigns are presented and discussed in Section IV. Finally, some concluding remarks are given.

## II. PLASMA SHAPE CONTROL AT JET

In this section we first give an overview of the JET Plasma Position and Current Control (PPCC) system. Afterwards the JET shape control system is introduced. For further details the interested readers can refer to [7] and [8].

The PPCC system is in charge of the axisymmetric magnetic control [9]. Indeed, when dealing with the control of the

G. De Tommasi, G. Ambrosino and A. Pironti are with the Assoc. EURATOM-ENEA-CREATE/Università di Napoli Federico II, Via Claudio 21, 80125, Napoli, Italy. detommas@unina.it.

M. Ariola is with Assoc. EURATOM-ENEA-CREATE/Università di Napoli Parthenope, Centro Direzionale di Napoli, Isola C4, 80143 Napoli, Italy.

G. Calabrò is with Assoc. EURATOM-ENEA, Frascati, Italy.

S. Galeani, G. Varano and R. Vitelli are with Dipartimento di Informatica, Sistemi e Produzione, Università di Roma, Tor Vergata, Rome, Italy.

F. Maviglia is with Assoc. EURATOM-ENEA-CREATE, Via Claudio 21, 80125, Napoli, Italy.

F. G. Rimini is with Euratom-CCFE, Culham Science Centre, OX14 3DB, Abingdon, UK.

A. C. C. Sips is with European Commission, B-1049 Brussels, Belgium.

L. Zaccarian is with CNRS, LAAS, 7 avenue du colonel Roche, F-31400 Toulouse, Univ. de Toulouse, LAAS, F-31400 Toulouse, France, and Dipartimento di Ingegneria Industriale, University of Trento, Italy.

*See the Appendix of F. Romanelli et al., Proceedings of the 24th IAEA Fusion Energy Conference 2012, San Diego, USA.
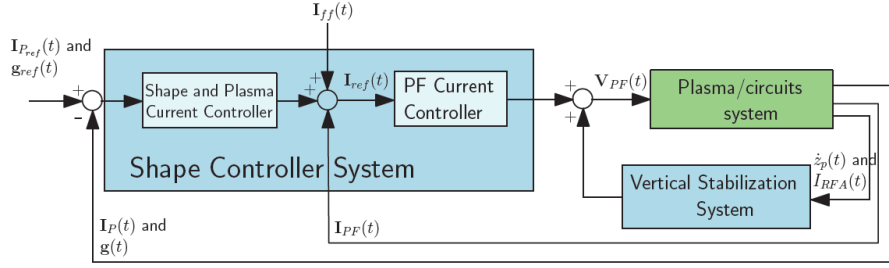
Fig. 1.   Simplified block diagram of the JET PPCC system.

current, position and shape of the plasma column inside the vacuum vessel, the problem is typically considered axisymmetric, and the following three control issues are considered: the vertical stabilization, the plasma shape control, and the plasma current control.

On almost all of the existing tokamaks, a frequency separation approach is adopted to solve the three aforementioned control problems. Following this approach, at JET the plasma is first vertically stabilized on a *fast* time scale, according to the constraints imposed by the passive structures and the actuator. Afterward, the current and shape controller is designed on the basis of the stable system obtained considering the presence of the vertical stabilization controller. In particular, for the JET tokamak, the time constant of the unstable mode is about 2 ms, while the settling time of the current and shape controller is about 0.7 s.

According to the frequency separation approach, the PPCC system has a distributed architecture that includes the following two subsystems

- the Vertical Stabilization (VS, [10]) system, which stabilizes the plasma by controlling the plasma vertical velocity;
- the Shape Control (SC) system, which controls both plasma current and shape (and hence also its position).

The actuators used by the PPCC system are the Poloidal Field (PF) coils, which are linked together into 10 circuits driven by independent power supplies, named *P1*, *P4*, *IMB*, *SHA*, *PFX*, *D1*, *D2*, *D3*, *D4* and *RFA*. In particular, the *P1* circuit is controlled by the SC system and enables both the plasma inductive formation and the control of the plasma current. Furthermore, the SC system controls also *P4*, *IMB*, *SHA*, *PFX*, *D1*, *D2*, *D3*, and *D4* to perform plasma shape control. The VS system stabilizes the plasma by controlling the current in the *RFA* circuit.

The block diagram in Fig. 1 shows both the VS and SC systems. The VS system stabilizes the plasma column by controlling to zero its vertical velocity $\dot{z}_p$.

Fig. 1 also depicts the internal structure of the SC system, showing its two main components, the *Shape and Plasma Current Controller* and the *PF Current Controller*.

The former computes the PF currents needed to counteract the disturbances and track the desired values for both the

plasma current $I_{P_{ref}}(\cdot)$ and of the plasma shape[1]. In the current implementation of the SC system, the user can choose two different algorithms for plasma shape control:

- the *standard Shape Controller* [8], which is conceived as a solution to the shape control problem for the entire discharge. During the plasma formation process, this algorithm controls the currents in the PF circuits so that they track a set of preprogrammed waveforms. Afterward, when a small plasma column is formed, only the plasma radial position is controlled. Eventually, during the main experimental phase, i.e. when the plasma becomes bounded by a separatrix ([11], see also the red curve in Fig. 2), the control is switched to the geometrical descriptors; in particular the standard Shape Controller gives the possibility of controlling simultaneously up to six geometrical descriptors. However the standard way to use it is to control up to four of the geometrical descriptors shown in Fig. 2 by dedicated control loops, while controlling the currents in the remaining PF coils.
- the XSC [1], which can be used only after the separatrix formation. This algorithm permits to perform a more precise tracking of the overall plasma shape, by simultaneously controlling, in a least squares sense, more than 30 geometrical descriptors.

The *PF Current Controller* is designed to control the current in each PF circuit. In particular, it receives as input the references for the PF currents $\mathbf{I}_{ref}$; these references are computed as the sum of two contributions:

- the feed-forward currents $\mathbf{I}_{ff}$ (also called *scenario* currents), i.e. the PF currents needed to achieve the target reference in terms of plasma current and shape;
- the feedback current requests computed by the *Shape and Plasma Current Controller*.

Based on the current control errors, the *PF Current controller* assigns the voltages to be applied to the PF coils.

## III.  THE JET EXTREME SHAPE CONTROLLER

This section briefly introduces the control algorithms of both the XSC and the CLA. The latter is an *additional feature*

---

[1]The plasma shape is usually specified via a vector of geometrical descriptors $\mathbf{shape}_{ref}(\cdot)$ that includes gaps, strike points and X-point positions (see also Tutorial 7 in [11]).
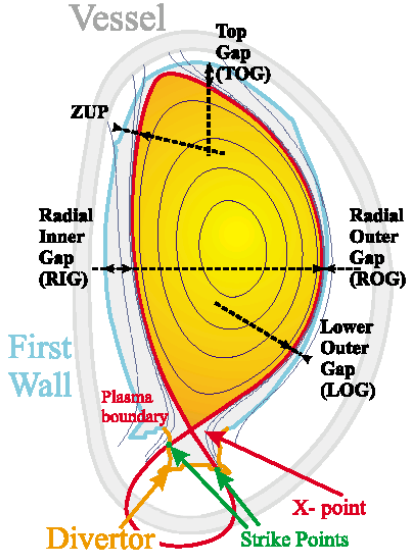
Fig. 2. Plasma shape descriptors that can be controlled by the JET standard Shape Controller.

that has been designed and implemented in 2011–2012 at JET, to prevent current saturation in the PF coils when the XSC is used to control the plasma shape. More details about the algorithms of the XSC and the CLA can be found in [1] and [5], respectively.

The XSC controls the whole plasma shape, specified as a set of geometrical descriptors (typically 32), calculating the PF coil current references. Its design [1] is based on the plasma linearized state space model [12], [13]. In particular, if $\delta\mathbf{g}$ are the $n_G(\leq 32)$ variations of the plasma shape descriptors, and $\mathbf{I}_{PF_N}$ are the PF currents normalized to the equilibrium plasma current, then

$$\delta\mathbf{g}(t) = \mathbf{C}\ \delta\mathbf{I}_{PF_N}(t)\,, \qquad (1)$$

which implies that the plasma boundary descriptors have the same dynamic response as the PF currents.

The XSC design is based on the matrix $\mathbf{C}$ in (1). It is worth to notice that the plant model is *non-right-invertible*, since $n_{PF} < n_G$, i.e., the number of independent control variables is less than the number of outputs to regulate. For such a plant it is not possible to track a generic set of references with zero steady-state error. Furthermore, given a generic set of references, the best performance that can be achieved in steady-state is to control to zero the error on $n_{PF}$ linear combinations of geometrical descriptors. Controlling to zero such an error is equivalent to minimizing the following steady-state performance index (see [2]):

$$J_1 = \lim_{t\to+\infty} (\delta\mathbf{g}_{ref} - \delta\mathbf{g}(t))^T (\delta\mathbf{g}_{ref} - \delta\mathbf{g}(t))\,, \qquad (2)$$

where $\delta\mathbf{g}_{ref}$ are *constant* references for the geometrical descriptors.

Minimization of (2) can be obtained by using the singular

value decomposition (SVD) of the matrix $\mathbf{C}$:

$$\mathbf{C} = \mathbf{U}\,\mathbf{S}\,\mathbf{V}^T\,,$$

where the matrix $\mathbf{S}$ contains the singular values, $\mathbf{U}$ and $\mathbf{V}$ are unitary matrices, that is

$$\mathbf{U}\,\mathbf{U}^T = \mathbf{U}^T\mathbf{U} = \mathbf{I}\,, \qquad \mathbf{V}\,\mathbf{V}^T = \mathbf{V}^T\mathbf{V} = \mathbf{I}\,.$$

As a matter of fact, using the JET linearized models, it turns out that some singular values (typically 2 or 3, depending on the configuration) are one order of magnitude smaller than the others.

This fact implies that minimizing the performance index (2) retaining all the singular values results in a large control effort at the steady state, in terms of PF coil currents. For this reason, the XSC achieves a trade-off condition, minimizing a modified quadratic cost function that penalizes both the error on the controlled shape descriptors, and the control effort. This is achieved controlling to zero the error only for the $\bar{n} < n_{PF}$ linear combination related to the largest 5 or 6 singular values [2].

The XSC design procedure does not take explicitly into account such saturation constraints; hence the PF currents may saturate during the experiment, triggering a safe stop procedure (*soft stop*).

In order to avoid PF current saturations when the XSC is used to control the plasma shape, the CLA system has been designed, implemented and successfully commissioned in 2011–2012 [6].
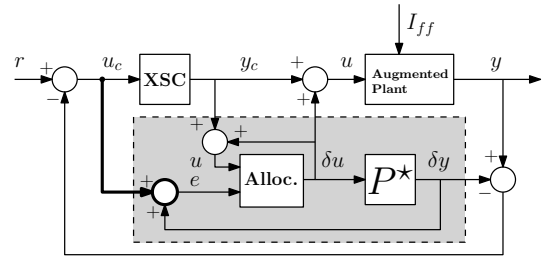


Fig. 3. Block diagram of the allocated closed-loop. The Current Limit Avoidance is the grey shaded box, and takes both the controller input and output signals as an input.

The CLA algorithm exploits the following idea: keep the PF currents within their limits without degrading too much the plasma shape, by finding an optimal trade-off between these two objectives.

In particular, the CLA aims at keeping the value of the plant inputs $\mathbf{u}$, i.e. the PF currents, inside a desirable region, meanwhile ensuring a small tracking error $\mathbf{e} = \mathbf{r} - \mathbf{y}$, i.e. a small error on the plasma shape. In order to quantify this trade-off, a continuously differentiable cost function $J_2(\mathbf{u}^\star, \mathbf{e}^\star)$ is introduced, where the superscript $\star$ on a signal denotes its steady-state value.

The CLA corresponds to the grey shaded box in Fig. 3, which received inputs from the XSC (block $XSC$ in Fig. 3) and modifies the request to the plant, i.e., the plasma controlled by the PF current controller

(block *Augmented Plant* in Fig. 3). If we denote by $\mathbf{x}_a \in \mathbb{R}^{n_a}$ the allocator internal state, and by $\mathbf{B}_0 \in \mathbb{R}^{n_{PF} \times n_a}$ a suitable full column rank matrix, then the two allocator outputs read

$$\delta\mathbf{u} = \mathbf{B}_0\mathbf{x}_a \,, \qquad (3)$$

and

$$\delta\mathbf{y} = \mathbf{P}^{\star}\mathbf{B}_0\mathbf{x}_a \,, \qquad (4)$$

where $\mathbf{P}^{\star}$ is the steady-state input/output gain of the plant. The output (3) modifies the PF current requests generated by the XSC, while (4) *hides* the resulting steady-state change in the plasma shape to the XSC. Hiding the plasma shape change to the XSC is required in order to prevent the controller to react to these changes. The allocator equations are given by

$$\dot{\mathbf{x}}_a = -\mathbf{K}\mathbf{B}_0^T \begin{bmatrix} \mathbf{I} \\ \mathbf{P}^{\star} \end{bmatrix}^T (\nabla J_2)^T \Big|_{(\mathbf{u},\mathbf{e})} \,, \qquad (5a)$$

$$\delta\mathbf{u} = \mathbf{B}_0\mathbf{x}_a \,, \qquad (5b)$$

$$\delta\mathbf{y} = \mathbf{P}^{\star}\mathbf{B}_0\mathbf{x}_a \,, \qquad (5c)$$

$$\mathbf{e} = \mathbf{r} - \mathbf{y} \,. \qquad (5d)$$

where $\mathbf{K} \in \mathbb{R}^{n_a \times n_a}$ is a symmetric positive definite matrix used to both specify the allocator convergence speed, and to distribute the allocation effort in the different directions.

The key property of the current allocator algorithm (5) is that, under suitable assumptions on the cost $J_2$, for each constant current request of the XSC, it has a unique globally asymptotically stable equilibrium $\mathbf{x}_a^{\star}$, coinciding with the unique global minimizer of $J_2$. It turns out that $J_2(\mathbf{u}^{\star}, \mathbf{e}^{\star})$ can be chosen in a suitable way in order to penalize the plasma shape error $\mathbf{e}^{\star}$ in addition to the PF currents $\delta\mathbf{u}^{\star}$.

## IV. EXPERIMENTAL RESULTS

This section describes the experimental results obtained during the 2012 JET experimental campaigns with the ITER-like beryllium wall.

In particular, we present the improvements that have been achieved in controlling the plasma shape by using the XSC during the plasma current ramp-up and ramp-down phases. During these two phases, the plasma shape is affected by several disturbances, i.e. plasma current variation itself and the variation of the plasma internal inductance $l_i$, which is related to the change of the current density internal profile. The XSC has been experimentally proven to behave better than the JET standard Shape Controller during both the plasma current ramp-up and ramp-down. It should be noticed that the full exploitation of the XSC during the ramp-down has been made possible thanks to the CLA, since in this phase the PF currents get close to their lower bounds (which are typically set equal to zero).

Furthermore, the XSC improved the plasma shape control performance also during the experiments aimed at studying the transition from low confinement (L-mode) to high confinement (H-mode) plasmas [14] during both current ramp-up and ramp-down [15]. In this case there is an additional disturbance that affects the shape, that is the variation of the poloidal beta $\beta_p$, which is related to the change of the plasma internal pressure due to the additional heating used to trigger the H-mode.

### A. Shape control during plasma current ramp-down

Let us first compare the behavior of the JET standard Shape Controller and of the XSC during the plasma current ramp-down. In order to perform this comparison let consider the following two JET pulses

- pulse #72203, which was controlled by the standard Shape Controller;
- pulse #83014, which was controlled by the XSC.

Figs. 6 and 7 show some plasma shape snapshots obtained by using the JET standard Shape Controller and the XSC, respectively. It is important to remark that, for pulse #72203, the standard Shape Controller was set to control the position of the two strike-points (see Fig. 2) by using the four divertor coils $D1$-$D4$, and the radial outer gap and the top gap (ROG and TOG in Fig. 2) with the $P4$ and $IMB$ circuits, respectively.
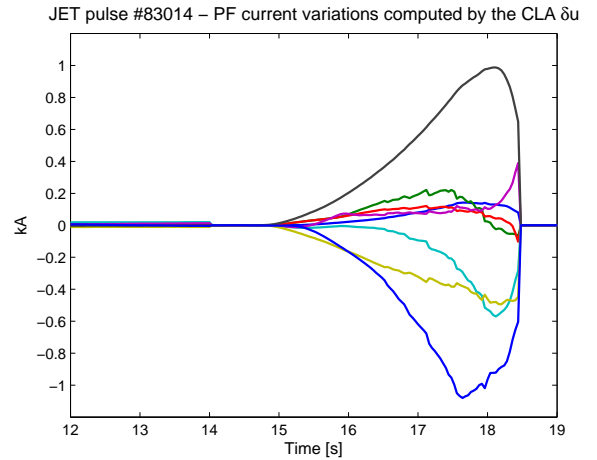


Fig. 4. Outputs of the CLA. This plot shows the PF current variations $\delta\mathbf{u}$ computed by the CLA and added to the XSC outputs.

From Fig. 6 it can observed that the standard Shape Controller poorly controls the inner side. This is mainly due to the fact that this controller uses the current in the $P4$ circuit (which mainly affects the plasma horizontal movement) to control the horizontal outer gap ROG with a SISO loop, without controlling the horizontal inner gap RIG (see Fig. 2). This poor control of the plasma inner side is reflected also in a bad control of the plasma top and X-point regions. Note that the control error for all the plasma descriptors controlled by the Shape Controller (i.e. ROG, TOG and the strike points) is kept very small, however the resulting overall plasma shape control is poor. Furthermore, after the considered ramp-down, $I_p$ is equal to $1\,MA$, thus the feedforward currents $\mathbf{I}_{ff}$ are still far from their lower bounds. Hence, in principle, there is still space to improve the shape control.
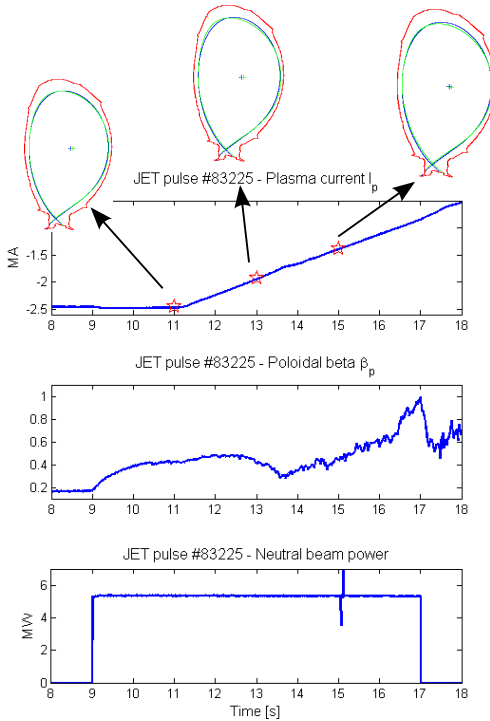
Fig. 5. Shape control with the XSC during the the L-H transition at the ramp-down (JET pulse #83225). In this figure the plasma shape is shown at different time instants during the ramp-down (the shape reference is the blue curve, while the green curve is the actual shape). The experimental values of the poloidal beta $\beta_p$ and of the neutral beam injected power are also shown.

Performance is indeed improved when the XSC controls the plasma, the overall shape control is improved, as shown in Fig. 7. In particular, the XSC achieves good tracking on both the inner and outer side, on the strike-points and on the X-point. The increase of the control error on the top region is mainly due to the CLA, which tries to prevent the PF currents from reaching their lower saturation limits by relaxing the plasma shape control. This is clearly shown by the CLA outputs shown in Fig. 4. In particular, the CLA outputs start to affect the plasma shape at $t \sim 16\ s$, and this effect becomes relevant at $t \sim 18\ s$. However, when the $I_p$ ramp-down is considered, reaching the saturation limits is unavoidable; indeed the soft stop is triggered at $t \sim 18.49$, causing XSC and CLA to lose the control (as shown by the sudden change of $\delta\mathbf{u}$ in Fig. 4).

Similar results have be obtained with the XSC during the L to H transitions while the plasma current is ramping down, as shown in Fig. 5. Here the XSC nicely controls the shape during the ramp-down also in the presence of $\beta_p$ variations due to the injected neutral beam heating power.

### B. Shape control during plasma current ramp-up

Fig. 8 shows the behavior of the XSC during the plasma current ramp-up of pulse #83014. In general, the same conclusions discussed in Section IV-A are valid also for the $I_p$ ramp-up case. However, it must be noticed that, since in this case the plasma current ramps up (in absolute value), the scenario feedforward $\mathbf{I}_{ff}$ move the PF currents away from their lower saturation limits. This implies that the CLA outputs are equal to zero. Hence, during the $I_p$ ramp-up, the CLA does not negatively affect the plasma shape control, and the XSC performance further improves with respect to the ramp-down case.

## CONCLUSIONS

After the successful implementation and commissioning of the CLA at the end of 2011, the XSC with CLA has been used for more the 200 pulses during the 2012 JET *ITER-like wall* campaigns. After having proved to be beneficial for the control of plasma shape during the plasma current ramp-up and ramp-down, the XSC has controlled the plasma during the ramp down phase of the last 151 pulses of the experimental campaign.

## REFERENCES

[1] M. Ariola and A. Pironti, "The design of the eXtreme Shape Controller for the JET tokamak," *IEEE Control Sys. Mag.*, vol. 25, no. 5, pp. 65–75, Oct. 2005.
[2] G. Ambrosino, M. Ariola, and A. Pironti, "Optimal steady-state control for linear non-right-invertible systems," *IET Control Theory Appl.*, vol. 1, no. 3, pp. 604–610, 2007.
[3] G. Ambrosino, M. Ariola, A. Pironti, and F. Sartori, "Design and implementation of an output regulation controller for the JET tokamak," *IEEE Trans. Contr. Sys. Tech.*, vol. 16, no. 6, pp. 1101–1111, Nov. 2008.
[4] W. Shi *et al.*, "Multivariable Robust Control of the Plasma Rotational Transform Profile for Advanced Tokamak Scenarios in DIII-D," in *Proc. of the American Control Conference*, Montréal, Canada, June 2012, pp. 5037–5042.
[5] G. De Tommasi, S. Galeani, A. Pironti, G. Varano, and L. Zaccarian, "Nonlinear dynamic allocator for optimal input/output performance trade-off: application to the JET Tokamak shape controller," *Automatica*, vol. 47, no. 5, pp. 981–987, May 2011.
[6] G. De Tommasi *et al.*, "First experimental results with the Current Limit Avoidance system at the JET tokamak," in *Proc.* 27th *Symposium on Fusion Technology (SOFT'12)*, Liège, Belgium, September 2012.
[7] M. Lennholm *et al.*, "Plasma control at JET," *Fus. Eng. Design*, vol. 48, no. 1–2, pp. 37–45, Aug. 2000.
[8] F. Sartori, G. De Tommasi, and F. Piccolo, "The Joint European Torus," *IEEE Control Sys. Mag.*, vol. 26, no. 2, pp. 64–78, Apr. 2006.
[9] M. Ariola and A. Pironti, *Magnetic Control of Tokamak Plasmas*. Springer, 2008.
[10] A. Neto *et al.*, "Exploitation of Modularity in the JET Tokamak Vertical Stabilization System," *Contr. Eng. Practice*, vol. 20, no. 9, pp. 846–856, Sep. 2012.
[11] A. Beghi and A. Cenedese, "Advances in Real-Time Plasma Boundary Reconstruction," *IEEE Control Sys. Mag.*, vol. 25, no. 5, pp. 44–64, Oct. 2005.
[12] R. Albanese and F. Villone, "The linearized CREATE-L plasma response model for the control of current, position and shape in tokamaks," *Nucl. Fus.*, vol. 38, no. 5, pp. 723–738, May 1998.
[13] R. Albanese, G. Calabrò, M. Mattei, and F. Villone, "Plasma response models for current, shape and position control at JET," *Fus. Eng. Des.*, vol. 66–68, pp. 715–718, 2003.
[14] R. Wolf, "Internal transport barrier in tokamak plasmas," *Plasma Phys. Control. Fus.*, vol. 45, no. 1, pp. R1–R91, Jan. 2002.
[15] G. Calabrò *et al.*, "H-mode and L-H threshold experiments during ITER-like plasma current ramp up/down at JET with ILW," in *submitted to* 40th *EPS conference on Plasma Physics*, Espoo, Finland, July 2013.
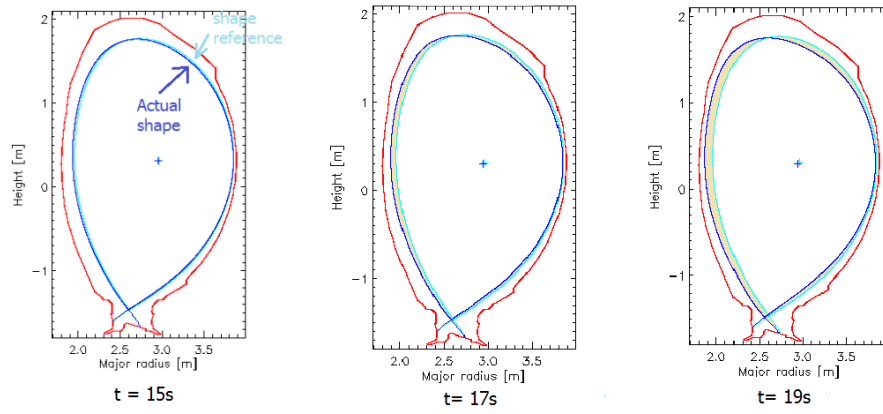
Fig. 6. Shape tracking with the JET standard Shape Controller during the plasma current ramp-down (pulse #77203).
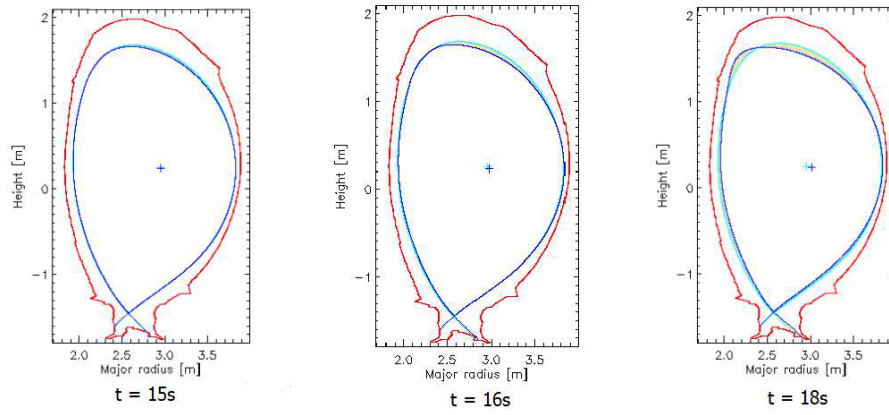


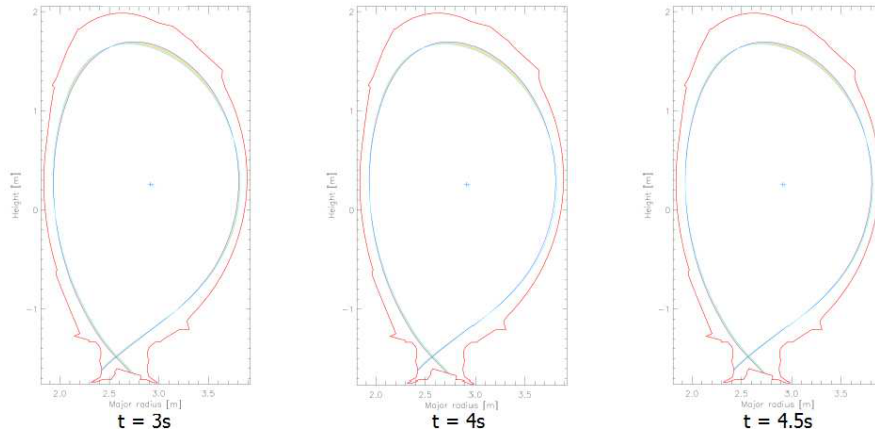Fig. 7. Shape tracking with the eXtreme Shape Controller during the plasma current ramp-down (pulse #83014).



Fig. 8. Shape tracking with the eXtreme Shape Controller during the plasma current ramp-up (pulse #83014).